

# AIAA'83

**AIAA-83-0125**

**Finite Element Formulations for Convection  
Dominated Flows With Particular Emphasis  
on the Compressible Euler Equations**

T.E. Tezduyar and T.J.R. Hughes,  
Stanford Univ., Stanford, CA

**AIAA 21st Aerospace Sciences Meeting**

January 10-13, 1983/Reno, Nevada

FINITE ELEMENT FORMULATIONS FOR CONVECTION DOMINATED FLOWS  
WITH PARTICULAR EMPHASIS ON THE COMPRESSIBLE EULER EQUATIONS

T.E. Tezduyar\* and T.J.R. Hughes\*\*  
Division of Applied Mechanics, Stanford University  
Stanford, California 94305

Abstract

A Petrov-Galerkin finite element formulation for first-order hyperbolic systems is developed generalizing the streamline-upwind approach which has previously been successfully applied to convection-diffusion and incompressible Navier-Stokes equations. The algorithm is applied to the Euler equations in conservation-law form and is shown to be effective in all cases studied, including ones with discontinuous solutions. Accurate and crisp representation of shock fronts in transonic problems is achieved.

1. Introduction

Analysis of inviscid, compressible fluid flows, especially ones with discontinuities, has been an interesting and challenging part of the research done in the field of computational fluid dynamics (see Lomax<sup>(1)</sup>). Currently, finite difference methods are widely used. However, these are difficult to apply to intricate geometries of aerodynamic interest. While the finite element method has not been extensively used in this area so far, there are potentially significant geometrical advantages.

In the finite element method, the problem domain is discretized into sub-domains (elements), and, via a weighted residual formulation, the governing differential equation system is translated into a system of ordinary differential equations.

In a weighted residual formulation, selecting the weighting functions from the same class that the interpolation functions are selected from, leads to a (Bubnov) Galerkin formulation. When applied to differential equation systems with symmetric operators (e.g. diffusion equations, most structural and solid mechanics problems) Galerkin formulations produce solutions with a "best approximation" property. That is, the error is minimized with respect to a certain norm.

For systems with non-symmetric operators (e.g. first-order hyperbolic systems), however, the Galerkin formulation does not possess a best approximation property. This, in some cases, may result in solutions with spurious node-to-node oscillations. In fact, this problem is not limited to Galerkin finite element formulations. It also arises for finite difference schemes when non-symmetric operators are approximated centrally.

Instead of using weighting functions which lead to a Galerkin formulation, one can employ a

Petrov-Galerkin formulation by modifying those weighting functions according to an optimal rule. The basic idea is to minimize the spurious oscillations without introducing excessive diffusion to the solution.

An optimal streamline upwind/Petrov-Galerkin formulation for convection dominated flows was recently developed by Hughes and Brooks<sup>(2,3,4)</sup> and was successfully applied to the solution of convection-diffusion and incompressible Navier-Stokes equations.

In this work we present a Petrov-Galerkin algorithm which is a generalization of the streamline upwind/Petrov-Galerkin algorithm to hyperbolic systems. The weighting functions (which would normally lead to a Galerkin formulation) are perturbed by the product of the coefficient matrix of the hyperbolic system, the gradient of the weighting function and a time parameter. By incorporating the coefficient matrix of the hyperbolic system into the weighting function we automatically inject the eigenvalue/eigenvector information of the system into our finite element formulation.

In section 2 we briefly describe the hyperbolic systems that we are concerned with, and in section 3 we introduce the Petrov-Galerkin formulation.

In section 4 the procedure of finite element discretization is defined.

In section 5 the selection of the time parameter, used in the Petrov-Galerkin formulation, is discussed.

Section 6 covers numerical applications with emphasis on problems with discontinuous solutions.

In section 7, we draw our conclusions and make suggestions for future research.

2. Initial/Boundary-value Problem

Let  $\Omega$  be an open region of  $\mathbb{R}^{n_{sd}}$ , where  $n_{sd}$  is the number of space dimensions, and let  $\Gamma$  and  $\bar{\Omega}$  denote its boundary and closure respectively. Spatial and temporal coordinates are denoted by  $\underline{x} = \{x_i\} \in \bar{\Omega}$  and  $t \in [0, T]$  respectively.

Consider the following system of  $m$  partial differential equations:

$$\underline{U}_{,t} + \underline{A}_{,j} \underline{U}_{,j} + \underline{G} = \underline{0} \quad (1)$$

where

$$\underline{U} = \underline{U}(\underline{x}, t) \quad (2)$$

\*Post-doctoral Research Engineer

\*\*Associate Professor of Mechanical Engineering

$$A_j = A_j(U, x, t) \quad 1 \leq j \leq n_{sd} \quad (3)$$

$$G = G(U, x, t) \quad (4)$$

$$U_{,j} = \partial U / \partial x_j \quad (5)$$

$$\tilde{A}_j U_{,j} = \sum_{j=1}^{n_{sd}} A_j U_{,j} \quad (\text{summation convention}) \quad (6)$$

Eq. (1) is said to be hyperbolic if for each  $k = \{k_j\} \in \mathbb{R}^{n_{sd}}$  there exists a transformation matrix  $\underline{S}$  such that

$$\underline{S}^{-1} (k_j A_j) \underline{S} = \underline{\Lambda} \quad (7)$$

where  $\underline{\Lambda}$  is a real, diagonal matrix.

Eq. (1) is called a balance law if there exist vectors  $\tilde{F}_j$  such that

$$A_j = \partial \tilde{F}_j / \partial U \quad 1 \leq j \leq n_{sd} \quad (8)$$

If, in addition to (8), we have that  $G = 0$ , (1) is called a conservation law.

Specification of appropriate boundary conditions for hyperbolic systems is a heavy task, especially in multi-dimensions. For a general treatment of this topic see Moretti (5) and Yee (6). For the present purposes, it suffices to assume that the boundary conditions take the abstract form

$$\partial U = g(t) \quad (9)$$

where  $\partial$  is a boundary operator and  $g$  is a prescribed function.

The initial/boundary-value problem for (1) consists of finding a function  $U$  which satisfies (1), the boundary conditions (9), and the following initial condition:

$$U(x, 0) = U_0(x) \quad (10)$$

where  $U_0$  is a given function of  $x \in \Omega$ .

### 3. Weighted Residual Formulation

Consider a discretization of  $\Omega$  into element subdomains  $\Omega^e$ ,  $e = 1, 2, \dots, n_{el}$ , where  $n_{el}$  is the number of elements. We assume

$$\bar{\Omega} = \bigcup_{e=1}^{n_{el}} \Omega^e \quad (11)$$

$$\phi = \bigcap_{e=1}^{n_{el}} \Omega^e \quad (12)$$

A weighted residual formulation of (1) is given by

$$0 = \int_{\Omega} \tilde{W} \cdot (U_{,t} + \tilde{A}_j U_{,j} + G) d\Omega \quad (13)$$

where  $\tilde{W}$  is a weighting function and  $\cdot$  denotes the dot product. In all cases we assume  $U$  is approximated by standard,  $C^0$ , finite element interpolations. The weighting functions may be selected from a different set of functions than the trial solutions. Thus (13) gives rise to a Petrov-Galerkin formulation. (2-4, 7-14)

An important class of Petrov-Galerkin methods, which is emphasized in the sequel, is defined by the following expression for  $\tilde{W}$ :

$$\tilde{W} = W + \tau_i W_{,i} \quad (14)$$

where  $W$  is a member of the same class of functions as the trial solutions and

$$\tau_i = \tau_i A_i^T \quad (\text{no sum}) \quad (15)$$

where  $\tau_i$  is a parameter which is chosen to optimize accuracy according to some criterion. This class of methods represents a generalization to hyperbolic systems of the streamline-upwind/Petrov-Galerkin formulation which has been successfully applied heretofore to the convection-diffusion and incompressible Navier-Stokes equations. (2,3,4)

The above choice of  $\tau_i$  has interesting consequences. For example, assume the one-dimensional, linear, constant-coefficient case in which  $G = 0$ . Then the one-dimensional counterpart of Eq. (13) reduces to the canonical form

$$0 = \int_{\Omega} (\bar{W} + \tau \bar{W}_{,x}) \cdot (\bar{U}_{,t} + \tau \bar{U}_{,x}) d\Omega \quad (16)$$

where  $\bar{W} = \underline{S}^T W$  and  $\bar{U} = \underline{S}^{-1} U$ . Thus (16) is equivalent to a system of uncoupled scalar equations. Scalar equations of this form are extensively analyzed in Tezduyar and Hughes. (15)

Furthermore, this choice, in one dimension, leads to difference equations which, under special circumstances, have essential features in common with the Lax-Wendroff method. (16)

If  $\tau_i$  is taken to be zero then we have the usual Galerkin method which possesses central-difference like character.

### 4. Semi-discrete Equations

Spatial discretization of the weighted residual equation (13) via finite elements leads to the following semi-discrete system of ordinary differential equations:

$$\dot{\underline{v}} + \underline{C} \underline{v} = \underline{F} \quad (17)$$

where  $\underline{M} = \underline{M}(\underline{v}, t)$  is the generalized "mass" matrix,  $\underline{C} = \underline{C}(\underline{v}, t)$  is the generalized convection matrix,  $\underline{F} = \underline{F}(\underline{v}, t)$  is the force vector,  $\underline{v}$  is the vector of (unknown) nodal values of  $U$ , and a superposed dot denotes time differentiation. The initial-value problem for (17) consists of finding a function  $\underline{v} = \underline{v}(t)$  satisfying (17) and the initial condition

$$\underline{v}(0) = \underline{v}_0 \quad (18)$$

where  $\nu_0$  is determined from (10).

The arrays in (17) are assembled from element contributions:

$$\tilde{M} = \mathbf{A} \sum_{e=1}^{n_{el}} (\tilde{m}^e) \quad (19)$$

$$\tilde{m}^e = [m_{ab}^e] \quad (20)$$

$$m_{ab}^e = \int_{\Omega^e} (N_a \underline{I} + N_{a,i} \underline{T}_i^T) N_b \, d\Omega \quad (21)$$

$$\tilde{C} = \mathbf{A} \sum_{e=1}^{n_{el}} (\tilde{c}^e) \quad (22)$$

$$\tilde{c}^e = [c_{ab}^e] \quad (23)$$

$$c_{ab}^e = \int_{\Omega^e} (N_a \underline{I} + N_{a,i} \underline{T}_i^T) A_i N_{b,j} \, d\Omega \quad (24)$$

$$\tilde{F} = \mathbf{A} \sum_{e=1}^{n_{el}} (\tilde{f}^e) \quad (25)$$

$$\tilde{f}^e = \{f_a^e\} \quad (26)$$

$$\tilde{f}_a^e = \int_{\Omega^e} N_a \underline{G} \, d\Omega - \sum_{b=1}^{n_{en}} (m_{ab}^e \underline{g}_b^e + c_{ab}^e \underline{g}_b^e) \quad (27)$$

where  $\mathbf{A}$  represents the finite element assembly operator;  $a$  and  $b$  are (local) element node numbers;  $1 \leq a, b \leq n_{en}$  where  $n_{en}$  is the number of nodes for the element under consideration;  $N_a$  is the element shape function associated with node  $a$ ;  $\underline{I}$  is the  $m \times m$  identity matrix; and  $\underline{g}_b^e$  is a vector which contains the boundary condition data emanating from (9). The dimensions of the nodal arrays  $m_{ab}^e$  and  $c_{ab}^e$  are  $m \times m$ , and the dimension of  $f_a^e$  and  $\underline{g}_b^e$  are  $m \times 1$ .

### 5. Selection of $\tau_i$

Three expressions for  $\tau_i$  have been experimented with. They are given as follows:

#### spatial criteria

We consider two multi-dimensional local criteria:

$$\tau_i = F \alpha h / \rho \quad 1 \leq i \leq n_{sd} \quad (28)$$

and

$$\tau_i = F \alpha h_i / \rho_i \quad (\text{no sum}) \quad 1 \leq i \leq n_{sd} \quad (29)$$

where  $\alpha$  is a transient algorithm parameter,  $F$  is a non-dimensional parameter and  $\rho_i$  is the spectral radius of  $A_i$ , that is,

$$\rho_i = \max_{1 \leq j \leq m} |\lambda_j(A_i)| \quad (30)$$

and

$$\rho = \|\underline{\rho}\| = (\rho_i \rho_i)^{\frac{1}{2}} \quad (31)$$

$$h = h_i \rho_i / \rho \quad (32)$$

$$h_i = 2 \|\nabla x_i\| \quad (33)$$

Eq. (33) holds for standard low-order isoparametric elements. The gradient operator,  $\nabla$ , is taken in terms of the natural Cartesian coordinates of the bi-unit  $n_{sd}$ -cube. For example, (33) yields the following formulas:

$$n_{sd} = 1 : h = 2 |\partial x / \partial \xi| \quad (34)$$

$$n_{sd} = 2 : h_i = 2 \left( \left( \frac{\partial x_i}{\partial \xi} \right)^2 + \left( \frac{\partial x_i}{\partial \eta} \right)^2 \right)^{\frac{1}{2}} \quad (35)$$

If other types of finite elements are employed, (33) needs to be suitably modified. Note that (28) and (29) are local specifications of  $\tau_i$  in that it depends upon the element geometry and eigenvalues of  $A_i$  which varies from point to point. Rationale for this form of  $\tau_i$  is provided by the following examples:

#### Examples

1. Consider the scalar model equation

$$U_{,t} + \lambda U_{,x} = 0 \quad (36)$$

where  $\lambda$  is assumed constant. Raymond and Garder (13) have shown that if

$$F \alpha = 1/\sqrt{15} \quad (37)$$

then the semi-discrete equations achieve fourth-order phase accuracy.

2. Consider the steady analog of (36) regularized by a diffusion term,

$$\lambda U_{,x} = \epsilon U_{,xx} \quad (38)$$

As  $\epsilon \rightarrow 0$ , the choice

$$F \alpha = \frac{1}{2} \quad (39)$$

leads to nodally exact solutions. The general case for the convection-diffusion equation is described in Hughes and Brooks. (2,3,4)

#### Remark

The preceding optimality conditions, (37) and (39), need to be altered for higher-order elements. For example, in the case of three-node quadratic elements (39) should be changed to  $F \alpha = \frac{1}{4}$ . (17) Throughout this work only low-order elements are

employed.

temporal criterion

In this case we assume

$$\tau_i = F \alpha \Delta t \quad 1 \leq i \leq n_{sd} \quad (40)$$

where  $\Delta t$  is the time step of the transient algorithm. Note that (40) is a global specification in that  $\Delta t$  is the same for all elements.

This choice, in one-dimension, with  $F = 1$  and  $\alpha = \frac{1}{2}$  and coupled with an explicit transient algorithm leads to a Lax-Wendroff type method. (15)

Remark

The factor,  $F$ , in (28) and (40) has been included to account for nonlinear effects. It has been our experience that a value of  $F$  greater than or equal to one needs to be employed to adequately handle shock-wave phenomena.

6. Numerical Applications

Isothermal flow in a nozzle

We consider one-dimensional isothermal flow in a nozzle with cross-sectional area varying along the axis. The governing balance law equations, provided by Lomax et al. (18), possess the following conservation variable, flux and source vectors:

$$\underline{U} = \rho A \begin{Bmatrix} 1 \\ u \end{Bmatrix} \quad (41)$$

$$\underline{F} = A \begin{Bmatrix} \rho u \\ \rho u^2 + \rho c^2 \end{Bmatrix} \quad (42)$$

$$\underline{G} = \begin{Bmatrix} 0 \\ -\rho c^2 A_{,x} \end{Bmatrix} \quad (43)$$

where  $\rho$ ,  $u$  and  $c$  are density, velocity and acoustic speed respectively.  $A$  is the cross-sectional area of the nozzle.

We present results for the case in which the nozzle cross-sectional area is

$$A(x) = 1.0 + \frac{(x - 2.5)^2}{12.5} \quad 0 \leq x \leq 5. \quad (44)$$

and the acoustic speed is

$$c = 1.0 \quad (45)$$

The flow is subsonic at the inlet and outlet. A shock front forms at  $x = 4$ . The exact solutions, which can be obtained by the integration of the square of the Mach number (in this case  $u^2$ ),

were provided by Lomax et al. (18)

For boundary conditions, density was specified at both ends of the nozzle.

We introduced the source term into the equation system in a transient fashion. That is instead of having the full value of the term  $A_{,x}$  at the beginning, we let it reach its full value gradually. This is done by taking  $A_{,x}$  as a linear function of time during an initial time interval at the end of which  $A_{,x}$  reaches its full value. The numerical  $A_{,x}$  can be expressed as follows:

$$\frac{(A_{,x})_{\text{NUMERICAL}}}{A_{,x}} = \begin{cases} n/n_{ti} & n < n_{ti} \\ 1 & n \geq n_{ti} \end{cases} \quad (46)$$

where  $n_{ti}$  denotes the number of time steps marking the end of the transition interval. For the problem solved,  $n_{ti} = 10$ .

The finite element mesh has 40 elements with element length of 0.125. We set the transient-algorithm parameter  $\alpha$  to unity and employed implicit time-stepping schemes with 2 iterations. Further details are presented in Tezduyar-Hughes (15). The time parameter  $\tau$  was chosen spatially and the time step was taken to be 0.5.

Figure 1 shows the results, for  $F = 1, 2, 5$  and  $10$ , which are in close agreement with the exact solution. There are very slight oscillations near the shock front for low  $F$ . For  $F = 1$  and  $F = 2$  the shock front is across only one element. The error in the shock location is about half an element length. As  $F$  increases, the shock front becomes smeared.

Entropy condition test problem

We tested our algorithm on a problem governed by the inviscid Burgers' equation

$$u_{,t} + \left(\frac{u^2}{2}\right)_{,x} = 0 \quad (47)$$

with initial condition shown in Figure 2, frame 0. The initial condition has a stable shock on each side of an unstable one.

The mesh has 40 elements with uniform element length of 1.0. The transient-algorithm parameter  $\alpha$  was set to 0.5. The parameter  $\tau$  was chosen spatially with  $F = 1.0$ . An implicit time-stepping scheme with two iterations was employed (15). Each frame in Figure 2 corresponds to a time step ( $\Delta t = 2.174$ ).

As time passes, the unstable shock collapses while the stable shocks merge and form a single stable one. The last frame attains the exact steady-state solution.

Flow around a thin biconvex airfoil

We consider the problem of a thin biconvex airfoil placed in a uniform flow field. The axis ( $x_1$ -axis) of the parabolic arc is aligned with the

direction of the uniform flow (non-lifting case). The parabolic arc bounding the airfoil is described by the following expression:

$$x_2 = \frac{b}{2} [1 - (2x_1)^2] \quad (48)$$

where  $b$  denotes the ratio of the maximum airfoil thickness to the cord length; we chose it to be 0.10.

The governing equations are the Euler equations. The conservation variables and flux vectors are

$$\underline{u} = \rho \begin{Bmatrix} 1 \\ u_1 \\ u_2 \\ e \end{Bmatrix} \quad (49)$$

$$\underline{F}_j = \begin{Bmatrix} u_j \rho \\ u_j \rho u_1 + \delta_{j1} p \\ u_j \rho u_2 + \delta_{j2} p \\ u_j (\rho e + p) \end{Bmatrix} \quad (50)$$

where  $\rho$ ,  $\underline{u}$  and  $p$  are density, velocity and pressure respectively; and  $\delta_{ij}$  is the Kronecker delta. The total energy per unit mass,  $e$ , is the sum of the internal and kinetic energies per unit mass. An equation of state relates the pressure to the other variables. That is:

$$p = p(\rho, i) \quad (51)$$

$$i = e - \frac{1}{2} |\underline{u}|^2 \quad (52)$$

where  $i$  is the internal energy per unit mass. If we have an ideal gas then the equation of state becomes:

$$p = (\gamma - 1) \rho i \quad (53)$$

Here  $\gamma$  is the ratio of the specific heats, which is taken to be 1.4. The acoustic speed is related to density and pressure by the equation

$$c^2 = \gamma p / \rho \quad (54)$$

#### Boundary conditions

The free stream parameters are taken to be

$$\rho_\infty = 1, \quad u_{2\infty} = 0, \quad e_\infty = 1. \quad (55)$$

The value of  $u_{1\infty}$  is set according to the following formula which depends on the specified value of the free stream mach number  $M_\infty$ :

$$u_{1\infty}^2 = \frac{M_\infty^2 \gamma (\gamma - 1) e_\infty}{M_\infty^2 \gamma (\gamma - 1) / 2 + 1} \quad (56)$$

Along the  $x_1$ -axis, away from the airfoil, we impose the following condition on  $u_2$ :

$$u_2 = 0, \quad x_2 = 0, \quad |x_1| > .5 \quad (57)$$

On the surface of the airfoil, the velocity vector must be perpendicular to the surface normal vector. This restriction can be expressed as:

$$\frac{u_2}{u_1} = \frac{dx_2}{dx_1} \quad (58)$$

Assuming that the airfoil thickness is small enough, such that the uniform flow field is perturbed only slightly,  $u_1$  can be approximated in (58) by its free stream value (see Leipmann and Roshko(19)):

$$\frac{u_2}{u_{1\infty}} = \frac{dx_2}{dx_1} \quad (59)$$

From (48) and (59), the boundary condition on the surface of the airfoil can then be expressed as

$$u_2 = -4b x_1 u_{1\infty}, \quad |x_1| \leq .5 \quad (60)$$

We study the problem for two different values of the free stream Mach number. The subcritical value  $M_\infty = 0.5$  results in a symmetric subsonic solution, while the supercritical value  $M_\infty = 0.84$  gives a transonic solution with a shock near  $x_1 = 0.3$ .

#### Finite element mesh and boundary conditions

The computational domain is shown in Figure 3. We utilize three finite element meshes with different overall sizes: the medium and fine meshes with  $L_1 = 3.5$ ,  $L_2 = 3.0$ , and the coarse mesh with  $L_1 = 2.0$ ,  $L_2 = 1.5$ . Each mesh has  $4N$  elements in the  $x_2$ -direction; in the  $x_1$ -direction, there are  $8N$  elements across the airfoil and  $4N$  elements each upstream and downstream. The number of nodal points are:  $(16N + 1) \times (4N + 1)$ , total, and  $(8N + 1)$  across the airfoil. For the coarse mesh  $N = 1$ , for the medium mesh  $N = 2$ , and for the fine mesh  $N = 4$ .

The meshes are shown in Figure 4; they are symmetric with respect to the  $x_2$ -axis.

At the left boundary we set  $\rho$ ,  $u_1$  and  $e$  to their free stream values. At the upper boundary, we impose the condition  $u_2 = 0$ , which can physically be interpreted as a channel wall. Furthermore, for the transonic case, we also impose the free stream boundary conditions at the upper boundary. Along the  $x_1$ -axis we take the boundary conditions of (57) and (60). Imposing the boundary condition of (60) along the  $x_1$ -axis instead of on the airfoil surface is a standard thin-airfoil approximation.

We used the temporal definition of the parameter  $\tau_i$  with  $F = 1$ . The transient-algorithm parameter  $\alpha$  was set to unity. Implicit methods with one iteration were employed. (15)

The steady boundary condition of (60) was implemented in the same way as for the nozzle problem. That is, during an initial time period of certain length, the airfoil thickness ratio was taken as a linear function of time, and at the end of this time period (4 time steps) it reached its steady-state value.

#### Subsonic case

We compare our results, at free stream Mach number 0.5, to the analytical solution<sup>(20)</sup> of the Cauchy-Riemann equations of the small-perturbation problem.

Figure 5 shows the analytical and finite element (medium and coarse mesh) solutions. The values of  $C_p(CP)$  and  $U_1(U)$  are plotted along the airfoil.

The time steps for the medium and coarse meshes were set to 0.23 and 0.46, respectively. The fine mesh was not used for this case, because even the coarse mesh results were very close to the analytical solution.

#### Transonic case

Figure 6 shows the finite element solutions at free stream Mach number 0.84. We employed the medium and fine meshes with time steps 0.40 and 0.20, respectively.

At the upper computational boundary, both channel and free stream boundary conditions were imposed. The difference in the location of the shock fronts, for these two cases, is about 6% of the chord length. This is to be expected, because the channel boundary condition results in increased Mach number at the upper computational boundary.

In this problem, the medium mesh performed almost as well as the fine mesh. One should also note that even the fine mesh is relatively coarse compared to most finite difference grids used for this type of problem.

Figure 7 shows the Mach contours for the fine mesh with channel boundary condition.

### 7. Conclusions

In this paper, a Petrov-Galerkin finite element algorithm for first-order hyperbolic equation systems was presented. The algorithms were tested on several problems involving solutions with shocks. Accurate solutions were obtained in all cases studied. The algorithms handled shocks very satisfactorily; the shock fronts were, for the most part, very crisp with minimal oscillations.

Overall, the finite element algorithms suggested here performed very well for problems with smooth and discontinuous solutions. The optimal selection of the time parameter,  $\tau_i$ , which

appears as a factor in the perturbation part of the weighting functions, needs further delineation. This needs to be pursued from the standpoint of nonlinearities and shocks which are, of course, prime concerns in solving the compressible Euler equations.

We believe that, with the recent advances in the development of Petrov-Galerkin algorithms, the finite element method has now become a viable alternative in computational fluid dynamics. However, the efficiency of finite element algorithms still needs to be improved, especially with respect to decreasing storage requirements. Recently, an "element-by-element" approach to the finite element formulation has been proposed by Hughes, Levit and Winget.<sup>(21,22)</sup> The preliminary results seem to be promising, particularly for problems with symmetric operators. Eventually, with the help of such new concepts, the finite element method can be expected to become an economically competitive and powerful analysis tool in the field of computational fluid dynamics.

#### Acknowledgments

We gratefully acknowledge the support of the California Institute of Technology and Stanford University. We would like to thank the Computational Fluid Dynamics branch of the NASA Ames Research Center, and especially H. Lomax for guidance and encouragement, and J. Barton, T. Holst and J. Steger for valuable suggestions.

#### References

1. H. Lomax, "Some Prospects for the Future of Computational Fluid Dynamics", Proceedings of the 5th AIAA Computational Fluid Dynamics Conference, June 1981, Palo Alto, California.
2. T.J.R. Hughes and A. Brooks, "Galerkin/Upwind Finite Element Mesh Partitions in Fluid Mechanics", pp. 103-112, in Boundary and Interfacial Layers - Computational and Asymptotic Methods, J.J.H. Miller (ed.), Boole Press, Dublin, 1980.
3. T.J.R. Hughes and A. Brooks, "A Theoretical Framework for Petrov-Galerkin Methods with Discontinuous Weighting Functions: Application to the Streamline Upwind Procedure", to appear in Finite Elements in Fluids, Vol. 4, R. H. Gallagher (ed.), J. Wiley and Sons.
4. A. Brooks and T.J.R. Hughes, "Streamline Upwind/Petrov-Galerkin Formulations for Convection Dominated Flows with Particular Emphasis on the Incompressible Navier-Stokes Equations", to appear in the Proceedings of FENOMECH '81 and Computer Methods in Applied Mechanics and Engineering.
5. G. Moretti, "A Physical Approach to the Numerical Treatment of Boundaries in Gas Dynamics", Proceedings of Numerical Boundary Condition Procedures Symposium, October 19-20, 1981 Ames Research Center, NASA, Moffet Field, California.

6. H. C. Yee, "Numerical Approximation of Boundary Conditions with Applications to Inviscid Equations of Gas Dynamics", NASA TM 81265, March 1981.
7. A. J. Baker, Research on Numerical Algorithms for the Three-Dimensional Navier-Stokes Equations, I. Accuracy, Convergence and Efficiency, Technical Report AFFDL-TR-79-3141, Wright-Patterson Air Force Base, Ohio, December 1979.
8. I. Christie, D. F. Griffiths, A. R. Mitchell and O. C. Zienkiewicz, "Finite Element Methods for Second Order Differential Equations with Significant First Derivatives", International Journal for Numerical Methods in Engineering, Vol. 10, 1389-1396, 1976.
9. J. E. Dendy, "Two Methods of Galerkin Type Achieving Optimum  $L^2$  Rates of Convergence for First Order Hyperbolics", SIAM Journal of Numerical Analysis, Vol. 11, pp. 637-653, 1974.
10. J. C. Heinrich, P. S. Huyakorn, O. C. Zienkiewicz and A. R. Mitchell, "An 'Upwind' Finite Element Scheme for Two-Dimensional Convective Transport Equation", International Journal for Numerical Methods in Engineering, Vol. 11, pp. 134-143, 1977.
11. T.J.R. Hughes and J. Atkinson, "A Variational Basis for 'Upwind' Finite Elements", IUTAM Symposium on Variational Methods in the Mechanics of Solids, Northwestern University, Evanston, Illinois, September, 1978.
12. K. W. Morton and J. W. Barrett, "Optimal Finite Element Methods for Diffusion-Convection Problems", in Boundary and Interior Layers - Computational and Asymptotic Methods, J.J.H. Miller (ed.) Boole Press, Dublin, pp. 134-148, 1980.
13. W. H. Raymond and A. Garder, "Selective Damping in a Galerkin Method for Solving Wave Problems with Variable Grids", Monthly Weather Review, Vol. 104, pp. 1583-1590, 1976.
14. L. B. Wahlbin, "A Dissipative Galerkin Method for the Numerical Solution of First Order Hyperbolic Equations", pp. 147-169 in Mathematical Aspects of Finite Elements in Partial Differential Equations, Carl de Boor, (ed.), Academic Press, New York, 1974.
15. T. E. Tezduyar and T.J.R. Hughes, "Development of Time-accurate Finite Element Techniques for First-order Hyperbolic Systems with Particular Emphasis on the Compressible Euler Equations", Report prepared under NASA-Ames University Consortium Interchange No. NCA3-OR745-104.
16. R. D. Richtmyer and K. W. Morton, Difference Methods for Initial-Value Problems, Interscience Publishers, New York, 1967.
17. S. Nakazawa, Ph.D. Thesis, University of Swansea, to appear.
18. H. Lomax et al., Private Communications, 1981-1982.
19. H. W. Liepmann and A. Roshko, Elements of Gasdynamics, J. Wiley and Sons, New York, 1957.
20. H. Lomax and E. D. Martin, "Fast Direct Numerical Solution of the Nonhomogenous Cauchy-Riemann Equations", Journal of Computational Physics, Vol. 15, No. 1, May 1974, pp. 55-80.
21. T.J.R. Hughes, I. Levit and J. Winget, "An Unconditionally Stable Element-by-Element Algorithm for Heat Conduction Analysis", to appear in Journal of the Engineering Mechanics Division, ASCE.
22. T.J.R. Hughes, I. Levit and J. Winget, "An Element-by-Element Solution Algorithm for Problems of Structural and Solid Mechanics", to appear in Computer Methods in Applied Mechanics and Engineering.

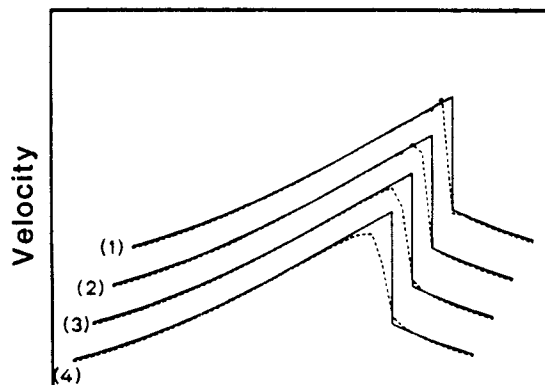
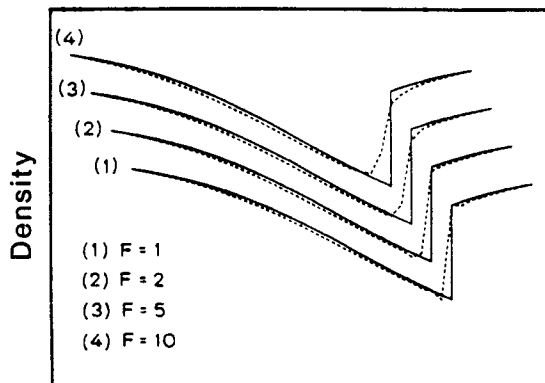


Figure 1 Isothermal flow in a nozzle: local  $\tau$ ,  $n_{e\ell} = 40$ .

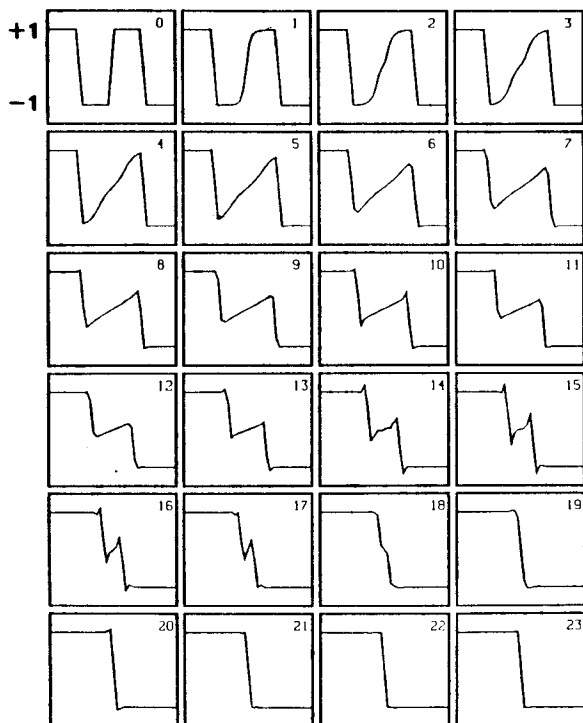


Figure 2 Entropy condition test problem:  
local  $\tau$ ,  $n_{el} = 40$ .

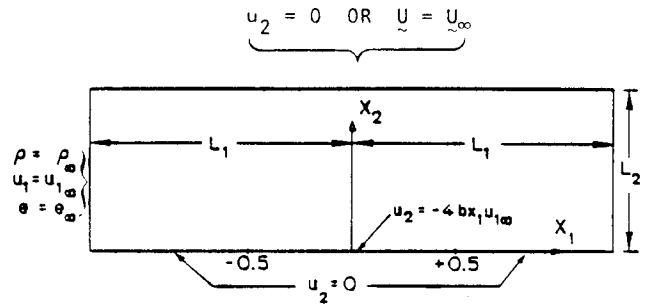


Figure 3 Flow around a thin biconvex airfoil:  
computational domain and boundary conditions.

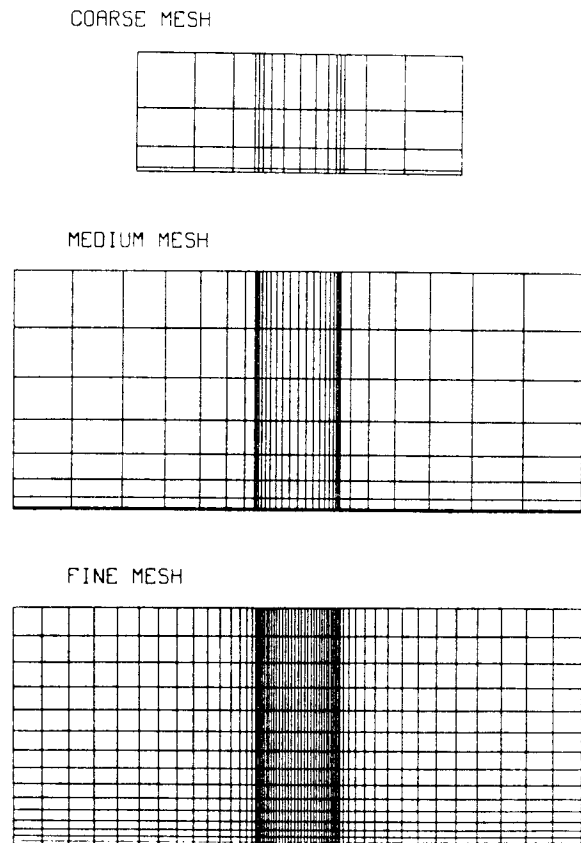


Figure 4 Flow around a thin biconvex airfoil:  
finite element meshes. Coarse mesh, 64 elements;  
medium mesh, 256 elements; fine mesh, 1016 elements.

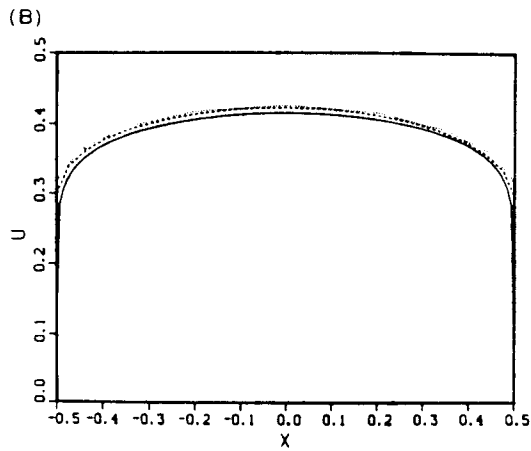
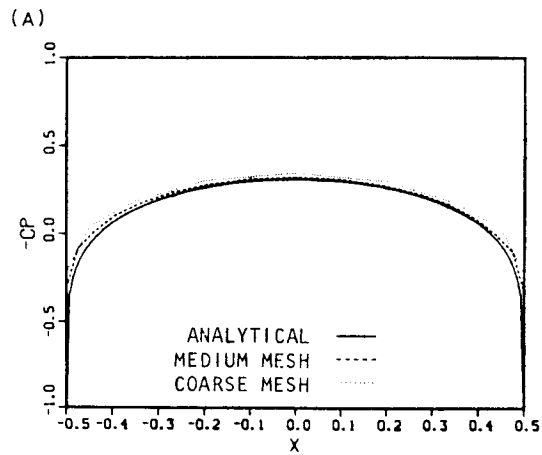


Figure 5 Flow around a thin biconvex airfoil, subsonic case:  $M_\infty = 0.50$ .

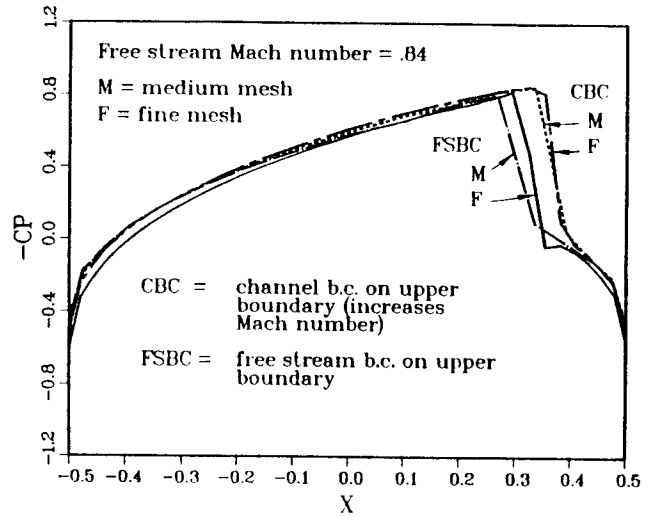


Figure 6 Flow around a thin biconvex airfoil, transonic case.

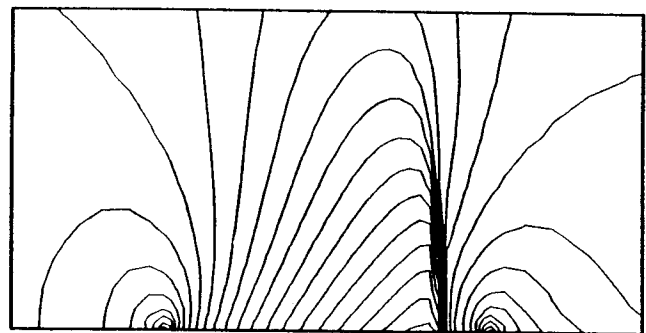


Figure 7 Flow around a thin biconvex airfoil, transonic case: Mach contours for fine mesh.